Title

Diffusion MRI changes in the anterior subventricular zone following chemoradiation in glioblastoma with posterior ventricular involvement

Journal

Journal of Neuro-Oncology, 147(3)

ISSN

0167-594X

Authors

Cho, Nicholas
Wang, Chencai
Raymond, Catalina
et al.

Publication Date

2020-05-01

DOI

10.1007/s11060-020-03460-5

Peer reviewed

HHS Public Access

Author manuscript

J Neurooncol. Author manuscript; available in PMC 2020 December 28.

Published in final edited form as:

J Neurooncol. 2020 May ; 147(3): 643–652. doi:10.1007/s11060-020-03460-5.

Diffusion MRI Changes in the Anterior Subventricular Zone Following Chemoradiation in Glioblastoma with Posterior Ventricular Involvement

Nicholas Cho[1,2,3], **Chencai Wang**[1,2], **Catalina Raymond**[1,2], **Tania Kaprealian**[4], **Matthew Ji**[5], **Noriko Salamon**[2], **Whitney B. Pope**[2], **Phioanh L. Nghiemphu**[5,6], **Albert Lai**[5,6], **Timothy F. Cloughesy**[5,6], **Benjamin M. Ellingson**[1,2,6]

[1]UCLA Brain Tumor Imaging Laboratory (BTIL), Center for Computer Vision and Imaging Biomarkers, David Geffen School of Medicine, University of California Los Angeles, Los Angeles, CA

[2]Department of Radiological Sciences, David Geffen School of Medicine, University of California Los Angeles, Los Angeles, CA

[3]Medical Scientist Training Program, David Geffen School of Medicine, University of California Los Angeles, Los Angeles, CA

[4]Department of Radiation Oncology, David Geffen School of Medicine, University of California Los Angeles, Los Angeles, CA

[5]Department of Neurology, David Geffen School of Medicine, University of California Los Angeles, Los Angeles, CA

[6]UCLA Neuro-Oncology Program, David Geffen School of Medicine, University of California Los Angeles, Los Angeles, CA

Abstract

Introduction: There is growing evidence that the subventricular zone (SVZ) plays a key role in glioblastoma (GBM) tumorigenesis. However, little is known regarding how the SVZ, which is a harbor for adult neural stem cells, may be influenced by chemoradiation. The current diffusion-weighted imaging (DWI) study explored ipsilateral and contralateral alterations in the anterior SVZ in GBM patients with posterior enhancing lesions following chemoradiation.

Methods: Forty GBM patients with tumor involvement in the posterior SVZ (mean age=57±10; left-hemisphere N=25; right-hemisphere N=15) were evaluated using DWI before and after chemoradiation. Regions-of-interest were drawn on the ipsilesional and contralesional anterior SVZ on apparent diffusion coefficient (ADC) maps for both timepoints. ADC histogram analysis was performed by modeling a bimodal, double Gaussian distribution to obtain ADC_L, defined as the mean of the lower Gaussian distribution.

Address Correspondence To: Benjamin M. Ellingson, Ph.D., Professor of Radiology, Biomedical Physics, Psychiatry, and Bioengineering, Director, UCLA Brain Tumor Imaging Laboratory (BTIL), Departments of Radiological Sciences and Psychiatry, David Geffen School of Medicine, University of California, Los Angeles, 924 Westwood Blvd., Suite 615, Los Angeles, CA 90024 (bellingson@mednet.ucla.edu), Phone: (310) 481-7572, Fax: (310) 794-2796.

Results: The ipsilesional SVZ had lower ADC_L values compared to the contralesional SVZ before treatment (mean difference=0.025 $\mu m^2/ms$; P=0.007). Following chemoradiation, these changes were no longer observed (mean difference=0.0025 $\mu m^2/ms$; P>0.5), as ADC_L values of the ipsilesional SVZ increased (mean difference=0.026 $\mu m^2/ms$; P=0.037). An increase in ipsilesional ADC_L was associated with shorter progression-free (P=0.0119) and overall survival (P=0.0265).

Conclusions: These preliminary observations suggest baseline asymmetry as well as asymmetric changes in the SVZ proximal (ipsilesional) to the tumor with respect to contralesional SVZ regions may be present in GBM, potentially implicating this region in tumorigenesis and/or treatment resistance.

Keywords

Diffusion weighted imaging; Apparent diffusion coefficient; Subventricular zone; Brain tumor; Glioblastoma; Radiation therapy

INTRODUCTION

Glioblastoma (GBM) is a highly-aggressive, malignant brain tumor that accounts for 52% of all primary brain tumor cases in the United States [1]. Prognosis for GBM patients is poor, and the median survival for patients is only around 15 months [2]. Currently, treatment for newly diagnosed GBM usually involves maximal surgical resection followed by chemoradiation including radiation therapy (RT) with concurrent temozolomide (TMZ) followed by adjuvant temozolomide. However, tumor recurrence remains unavoidable [3], suggesting resistance to chemoradiation may be inherent or acquired and may originate in the tumor microenvironment and/or the central nervous system as a whole.

Recent studies have implicated the subventricular zone (SVZ) in both GBM tumorigenesis and resistance to chemoradiation. GBMs are known to contain glioma stem cells that allow for self-renewing capability and intra-tumor heterogeneity, and the SVZ is known as one of the few brain regions that contains adult neural stem cells and has been suggested as a potential site for neurogenesis [4–6]. Lee *et al.* discovered genetic mutations within SVZ neural stem cells in high concentrations in GBM, providing the first direct genetic evidence for a potential SVZ origin of GBM [7]. Moreover, in a study of 507 GBM patients, 91.9% of GBMs were found to have some subventricular involvement, showing T2 hyperintensity and/or contrast enhancement extending into the periventricular white matter regions adjacent to the SVZ [8]. Injected GBM cells have also been shown to specifically infiltrate the SVZ in mouse models [9]. Additionally, irradiation of the SVZ has been associated with improved outcomes for GBM patients [10, 11], further suggesting a potential link between the SVZ, GBM tumorigenesis, and chemoradiation resistance.

One potential tool for investigating the SVZ microenvironment is diffusion-weighed imaging (DWI). DWI is a non-invasive imaging method commonly used to evaluate the cancer microenvironment directly; however, it may also provide insight into microstructural changes within the SVZ. The apparent diffusion coefficient (ADC), a quantity derived from DWI that reflects the relative mobility of water molecules, has been shown to be inversely

proportional to tumor or neural cell density [12–14] and the density of proliferating cells [15]. ADC has been used extensively as a biomarker in brain tumors for predicting survival, RT efficacy, and to explore distal structural changes in GBM patients as a result of long-term radiation damage [16–19]. However, despite a single conference abstract showing hemispheric differences in ADC values within the SVZ [20] and a single study on SVZ changes during chemoradiation [21], little is known about diffusion changes within the distal SVZ before and after chemoradiation in newly diagnosed GBM.

The purpose of the current study was to examine and quantify ADC changes in the SVZ of newly diagnosed GBM patients before and after chemoradiation. Using ADC histogram analysis to model the bimodal behavior of ADC within the SVZ, we hypothesized ADC_L values, the mean ADC of the lower Gaussian distribution, within ipsilesional SVZ (same hemisphere as the tumor) may be lower than the contralesional SVZ (opposite hemisphere from the tumor) prior to radiation, consistent with a higher cell density and/or proliferation rate of stem cells within the SVZ proximal to the tumor. Additionally, we hypothesized ADC_L within the ipsilesional, more proximal SVZ region may increase following chemoradiation, implying either a morphometric change in the SVZ cells or reduction in cellularity from either destruction of SVZ cells or migration of SVZ cells to the tumor site.

METHODS

Patient Selection

All patients participating in this study signed institutional review board-approved informed consent. Data acquisition was performed in compliance with all applicable Health Insurance Portability and Accountability Act regulations. Patients were retrospectively selected from our institution’s neuro-oncology database. A total of 40 patients who met the following criteria were selected: (1) pathology-confirmed glioblastoma; (2) tumor involvement in the posterior SVZ; (3) treatment with standard external beam radiotherapy (RT) and concurrent temozolomide (TMZ) followed by adjuvant TMZ, and (4) MRI scans obtained after surgical resection and within 4 weeks after completion of chemoradiation. The average age for this population was 57±10 years (S.D.), the average Karnofsky performance status (KPS) score was 90, and 65% were male (26/40). Of these 40 patients, 25 patients had tumor with left hemispheric involvement while 15 had right hemispheric involvement. Median progression-free survival (PFS) and overall survival (OS) from the end of chemoradiation for this patient population was 265 days and 622 days, respectively. Patient data are summarized in Table 1.

Magnetic Resonance Imaging

Diffusion and structural MRIs were obtained on GE Signa Excite HDx (GE Healthcare, Waukesha, WI); Siemens Symphony, Avanto, or Sonata 1.5T (Siemens Healthcare, Erlangen, Germany); or Siemens Trio or Verio 3T MRI system. Anatomical MRI, including pre-contrast axial T2-weighted images, fluid-attenuated inversion recovery (FLAIR) images, and pre- and post-contrast (gadolinium-diethylenetriamine pentacetic acid at a dose of 0.1 mmoL/kg body weight; Magnevist, Bayer Schering Pharma, Leverkusen, Germany) T1-weighted images were collected according to the international standardized brain tumor imaging protocol (BTIP)[22]. Additionally, each patient also received diffusion-weighted

images (DWIs) with echo time (TE) of 73–137 ms, repetition time (TR) of 3000–12000ms, slice thickness of 3–5mm with no interslice gap, matrix size of 128×128 or 192×192, number of excitations (NEX) of 1–4, flip angle of 90°, and b values of 0 and 1000 s/mm^2 in 3 orthogonal directions. ADC was calculated from the acquired b=0 s/mm^2 and b=1000 s/mm^2 DWIs.

Subventricular Zone ADC Histogram Analysis

All data was analyzed using Analysis of Functional NeuroImages (AFNI) software [23]. Regions-of-interest (ROIs) were manually drawn on all axial DWI scans prior to and following chemoradiation. ROIs were drawn separately on the anterior contralesional and ipsilesional SVZ using a 5-mm margin as described previously (Fig. 1A–B) [24]. ADC histogram analysis was then performed to remove possible contamination of cerebrospinal fluid by first extracting ADC values from each ROI, then fitting the ADC distribution to a double Gaussian mixed model (Fig. 1C),
$p(ADC) = f \cdot N\left(\mu_{ADC_L}, \sigma_{ADC_L}\right) + (1 - f) \cdot N\left(\mu_{ADC_H}, \sigma_{ADC_H}\right)$, where ADC_L and ADC_H represent the mean ADC value of the lower and higher Gaussian distribution, respectively [16, 25, 26]. ADC_L values within each region of the SVZ were retained and used for comparison.

Determination of Disease Progression

Progression was defined prospectively by the treating neuro-oncologists if subsequent scans showed an increase in imaging-evaluable tumor (≥25% increase in the sum of enhancing lesions, new enhancing lesions > 1 cm^2, or an unequivocal qualitative increase in nonenhancing tumor). Patients who required an increased dosage of steroids to maintain neurologic function, even when anatomical images showed no worsening, were considered to be stable but received more frequent MRI evaluation. Patients who experienced significant neurologic decline were also declared to have progressed at the time of irreversible decline. PFS was defined as the time between the end of concurrent TMZ and RT until disease progression. OS was defined as the time from end of concurrent TMZ and RT until death or until the last record of clinical evaluation.

Statistical Analyses

All statistical tests were performed using SPSS software version 25.0 (IBM SPSS Institute Inc, Chicago, IL) or GraphPad Prism v7.0e (San Diego, CA). Significance level was set at α=0.05 and all tests were two-tailed. Paired t-tests were conducted to compare differences between pre- and post-RT ADC_L values for the contralesional and ipsilesional SVZ and between contralesional and ipsilesional SVZ ADC_L values at the same timepoint. Pearson correlation analysis was performed to assess relationships between the ADC_L values and clinical variables (days between scans, age, and survival).

RESULTS

Most patients showed a characteristic increase in ADC within the SVZ following completion of chemoradiation (Fig. 2A–B), consistent with previous studies examining changes within the tumor bed itself [21, 27, 28]. However, prior to any chemoradiation, the anterior aspect

of the ipsilateral SVZ had a 72% lower ADC_L compared with the anterior aspect of the contralesional SVZ (Fig. 2C,E; *P=0.0067*). Interestingly, this asymmetry was no longer present after completion of chemoradiation (Fig. 2D,F; *P=0.6808*), with the contralesional SVZ having only a 7% higher ADC_L. In patients with left hemispherical tumor involvement (*N=25* of *40*), the ipsilesional SVZ had significantly lower ADC_L compared with the contralesional SVZ prior to chemoradiation (ΔADC_L = 0.036 μm^2/ms, *P=0.007*). No asymmetry in ADC_L was observed in patients with right hemispheric tumor involvement, nor were any differences observed in either patient cohort following completion of chemoradiation (*P>0.5*).

Within the ipsilesional SVZ, ADC_L increased an average of 3.3% (ΔADC_L = 0.026 μm^2/ms) after administration of chemoradiation (Fig. 3A–B; *P=0.0373*), with 57.5% of patients exhibiting an increase in ADC_L (Fig. 3C). This was particularly interesting because the contralesional SVZ did not demonstrate much of a change ADC_L after chemoradiation (Fig. 3D–E; *P=0.6929*), averaging a 0.6% increase in ADC_L and around 47.5% of patients showing any increase in ADC_L in this region (Fig. 3F). These trends seem to be driven mostly by patients with left hemispheric tumor involvement (Supplemental Figure S1; *N=25* of the 40 patients), with an ADC_L increase of 0.041 μm^2/ms (*P=0.017*) in the ipsilateral SVZ following chemoradiation. No difference in ADC_L within the contralesional SVZ was observed (*P>0.5*).

A significant positive association was observed between patient age and change in ADC_L in both the ipsilesional (Fig. 4A; R^2*=0.2006, P=0.0038*) and contralesional SVZ (Fig. 4B; R^2*=0.1432, P=0.0161*). Patient age was also correlated with post-chemoradiation ADC_L measurements for both ipsilesional (R^2*=0.2601, P=0.001*) and contralesional SVZ (R^2*=0.2025, P=0.004*).

An increase in ADC_L within the anterior ipsilesional SVZ following chemoradiation resulted in a significantly shorter PFS compared with patients exhibiting a decrease in ADC_L (Fig. 4C; *Log-rank, P=0.0244, Hazard Ratio (HR) = 2.043 [95% C.I. = 1.138 – 4.163], median PFS = 21.7 vs. 55.2 days*). Similarly, patients with a measurable increase in ADC_L within the ipsilesional SVZ following chemoradiation had a significantly shorter OS (Fig. 4D; *Log-rank, P=0.0308, HR = 1.948 [1.119–4.114]*). The observation was still significant for PFS after accounting for age, tumor hemisphere, and the interaction between hemisphere and change in ADC_L (Table 2; *Cox multivariable regression, P=0.0237*). However, change in ADC_L was not a significant predictor of OS after accounting for these other variables (Table 3; *Cox multivariable regression, Change in* ADC_L*, P=0.1689*), but tumor hemisphere was a significant predictor OS (*P=0.0281*).

DISCUSSION

There is a growing body of evidence implicating the migration of neural stem cells from the SVZ during GBM tumorigenesis and resistance to chemoradiation [7–11]. In the present study, ADC_L measurements in the ipsilesional SVZ prior to chemoradiation were lower than the contralesional SVZ, which appears consistent with findings in a previous pilot study demonstrating lower diffusion kurtosis in the ipsilesional SVZ [20]. Lower ADC values are

traditionally thought to reflect increased cellular density [12] or higher proliferation [15], so the present findings may suggest higher neural stem cell density or heightened cellular proliferation in the SVZ regions proximal to the tumor. This is also consistent with the interpretation of diffusion characteristics in the SVZ of cognitively-impaired and Alzheimer's disease patients, where Cherubini *et al.* suggested higher ADC values in the SVZ was due to reduced neurogenesis [29]. Increased SVZ neurogenesis on the ipsilesional side proximal to the tumor is also consistent with previous reports on genetic similarities between GBM cells and ipsilesional SVZ cells [7], and the observation of ipsilesional SVZ involvement on MRI in 90% of GBM patients [8].

The current study observed a significant increase in ADC_L within the ipsilesional SVZ following chemoradiation, but no change in ADC_L within the contralesional SVZ. This finding is in line with a previous study that observed increasing ADC values in the SVZ during chemoradiation for GBM [21]. Moreover, results showed a reduction in asymmetry in ADC_L between the ipsilesional and contralesional SVZ after chemoradiation. Since ADC_L characteristics in the contralesional SVZ remained virtually unchanged after chemoradiation, the rise in ADC_L values within the ipsilesional SVZ may suggest that chemoradiation may change the morphometry, reduce cell density, and/or reduce neural stem cell neurogenesis through altered migration or direct destruction of cells within the SVZ. Previous studies have shown that direct irradiation of the SVZ impairs neural stem cell migration [30] and is associated with improved patient outcomes [10, 11]. Irradiation of the hippocampus, another site of neurogenesis in the adult human brain, has also been shown to reduce long-term neurogenesis [31]. Thus, it is conceivable that direct or indirect irradiation of the proximal, ipsilesional SVZ during treatment of the tumor may lead to changes in ADC reflecting tumor cell destruction and inhibition of neurogenesis within the tumor bed as well as the distal, ipsilesional SVZ, respectively. Alternatively, the increase in ADC_L in the distal, ipsilesional SVZ after chemoradiation may indicate migration of stem cells from the SVZ to the site of the tumor in order to recapitulate the original tumor hierarchy [32], possibly resulting in lower cellular density of distal SVZ portions. This appears consistent with our current observations, in that patients with a significant increase in ADC_L in the distal, ipsilesional SVZ tended to have shorter PFS and OS. One possible explanation is that increased cellular migration from the distal, ipsilesional SVZ to the tumor bed may have resulted in the increased ipsilesional SVZ ADC_L values, leading to increased tumor recapitulation and worsened OS and PFS—however, this is purely speculative. Of note, after controlling for age and hemispheric involvement, both of which showed associations with diffusivity measurements in the SVZ, these trends with respect to PFS and OS were no longer statistically significant. Future, well-controlled studies with a larger number of patients that also include colocalization of radiation treatment plans would be beneficial for determining the origin of possible dose-dependent changes in ADC_L within the SVZ and the precise implications on patient outcome. These studies may also want to assess ADC differences between proximal and distal SVZ regions for potential heterogenous impacts of chemoradiation on the SVZ and their association with patient prognosis.

It is worth noting that the primary trends appeared to be isolated to patients with left-hemispheric tumors, but not in patients with right-hemispheric lesions. Of course, one potential explanation for this is the fact that right-hemispheric tumor patients (N=15)

compared to left-hemispheric tumor patients (N=25) were smaller in sample size in the current study. Future studies with more patients will have to control for left and right-hemispheric tumors to accurately assess if there are true hemispheric differences in SVZ changes. Interestingly, studies have also shown differences in patient outcome dependent on tumor location, with patients harboring right-hemispheric tumors involving the SVZ exhibiting shorter overall survival compared to left-hemispheric tumors [8]. The current study was not consistent with these previous observations, showing patients with left-hemispheric tumors having shorter OS (Supplemental Figure S2; *PFS, Log-rank, P=0.2004; OS, P=0.0079*). However, it is important to note the current study only considered posterior lesions and those contiguous with the SVZ, so these observations may not be generalizable across all tumor locations within a particular hemisphere, or even throughout the SVZ. Future studies with more patients will be required to determine the possible prognostic role of tumor location combined with changes in SVZ ADC_L following chemoradiation.

In addition to tumor location, older patient age was also associated with a higher increase in ADC_L following chemoradiation for anterior regions in both the ipsilesional and contralesional SVZ, suggesting that age may play a pivotal role in both chemoradiation sensitivity and in neurogenesis of the SVZ. For example, older patients demonstrate greater and more widespread white matter changes following whole-brain radiation therapy compared with younger patients [33]. Preclinical studies have shown decreased neurogenesis in the SVZ with increasing age, which was associated with reduced plasticity and age-related cognitive impairment [34]. Thus, older patients in the present study may demonstrate greater changes in ADC_L within the SVZ because of increased sensitivity to chemoradiation and/or reduced capacity for neurogenesis following therapy. The fact the association between age and change in ADC_L was observed in both hemispheres of the SVZ—not just the ipsilesional—further suggests this result may be due to age-related brain changes and not only from proximal effects of the encroaching tumor.

Limitations and Future Considerations

A confound to the current study, in addition to the limited study population size, is the use of relatively low-resolution DWI scans for the analysis. Inaccuracies in defining ROIs near the SVZ can lead to errors in ADC measurement due to partial volume effects between the SVZ tissue and the adjacent cerebrospinal fluid [35]. In order to overcome this limitation, we chose to model the underlying ADC histogram in the SVZ ROIs using a bimodal, double Gaussian model to accurately assess the diffusivity in the tissue compartment, or ADC_L. In addition, it is conceivable that different tumors received variable doses of radiation to the SVZ. As mentioned previously, future studies utilizing colocalization of radiation treatment plans will be required to determine possible dose-dependent changes in ADC_L within the SVZ. Additionally, given the association between radiation field and tumor size, future studies examining the association between tumor size, radiation field or dose, and resulting change in the SVZ are also warranted.

Molecular features of the tumor, including IDH mutation status and MGMT promoter methylation status, also impact patient prognosis [36, 37], but unfortunately this data was unavailable for all patients in the current study and therefore was not adequately powered to

address this question. Although we do not hypothesize chemoradiation-induced changes in the SVZ to differ between tumor subtypes, future studies should consider the impacts of molecular signatures on distal SVZ changes.

When determining PFS, it is also possible that some patients were deemed as exhibiting tumor progression when in fact they exhibited pseudoprogression, which can be difficult to differentiate using conventional MRI techniques. However, due to the retrospective nature of the current study, progression was determined prospectively consistent with clinical care practices during the particular time frame and patients were often changed to another therapy before radiographic confirmation of progression was obtained.

Additionally, diffusion MR measurements were obtained from a number of MR systems, vendors, and field strengths, which may have resulted in measurement inaccuracies. Future studies using a temperature-controlled water phantom could potentially address systemic variability across MR systems [38]. Lastly, multiple timepoints during chemoradiation and more sophisticated longitudinal modeling may provide more insights into the dynamic changes in the SVZ, tumor, and normal brain as a result of chemoradiation.

CONCLUSION

In newly diagnosed GBM patients with posterior lesions, the anterior ipsilesional SVZ has a lower diffusivity compared with the anterior contralesional SVZ, which normalizes following chemoradiation due to a significant increase in diffusivity within the ipsilesional SVZ. This plasticity observed in the more proximal regions of the SVZ to the tumor site may implicate the SVZ in gliomagenesis and/or chemoradiation sensitivity, as patients with an increase in diffusivity showed a shorter PFS and OS following chemoradiation.

Supplementary Material

Refer to Web version on PubMed Central for supplementary material.

Acknowledgements:

Funding: This study was funded by the National Institute of Health (NIH): NIH-NIGMS Training Grant GM008042 (Cho), American Cancer Society (ACS) Research Scholar Grant (RSG-15-003-01-CCE) (Ellingson); American Brain Tumor Association (ABTA) Research Collaborators Grant (ARC1700002)(Ellingson); National Brain Tumor Society (NBTS) Research Grant (Ellingson, Cloughesy); NIH/NCI UCLA Brain Tumor SPORE (1P50CA211015-01A1) (Ellingson, Lai, Cloughesy, Nghiemphu); NIH/NCI 1R21CA223757-01 (Ellingson)

REFERENCES

1. de Robles P, Fiest KM, Frolkis AD, Pringsheim T, Atta C, St Germaine-Smith C, Day L, Lam D, Jette N (2015) The worldwide incidence and prevalence of primary brain tumors: a systematic review and meta-analysis. Neuro Oncol 17: 776–783 doi:10.1093/neuonc/nou283 [PubMed: 25313193]
2. Koshy M, Villano JL, Dolecek TA, Howard A, Mahmood U, Chmura SJ, Weichselbaum RR, McCarthy BJ (2012) Improved survival time trends for glioblastoma using the SEER 17 population-based registries. J Neurooncol 107: 207–212 doi:10.1007/s11060-011-0738-7 [PubMed: 21984115]
3. Stupp R, Mason WP, van den Bent MJ, Weller M, Fisher B, Taphoorn MJB, Belanger K, Brandes AA, Marosi C, Bogdahn U, Curschmann J, Janzer RC, Ludwin SK, Gorlia T, Allgeier A, Lacombe D, Cairncross JG, Eisenhauer E, Mirimanoff RO (2005) Radiotherapy plus Concomitant and

Adjuvant Temozolomide for Glioblastoma. New England Journal of Medicine 352: 987–996 doi:10.1056/NEJMoa043330

4. Sanai N, Tramontin AD, Quinones-Hinojosa A, Barbaro NM, Gupta N, Kunwar S, Lawton MT, McDermott MW, Parsa AT, Manuel-Garcia Verdugo J, Berger MS, Alvarez-Buylla A (2004) Unique astrocyte ribbon in adult human brain contains neural stem cells but lacks chain migration. Nature 427: 740–744 doi:10.1038/nature02301 [PubMed: 14973487]
5. Mistry AM (2019) On the subventricular zone origin of human glioblastoma. Transl Cancer Res 8: 11–13 doi:10.21037/tcr.2018.11.31 [PubMed: 30873355]
6. Quinones-Hinojosa A, Sanai N, Soriano-Navarro M, Gonzalez-Perez O, Mirzadeh Z, Gil-Perotin S, Romero-Rodriguez R, Berger MS, Garcia-Verdugo JM, Alvarez-Buylla A (2006) Cellular composition and cytoarchitecture of the adult human subventricular zone: a niche of neural stem cells. J Comp Neurol 494: 415–434 doi:10.1002/cne.20798 [PubMed: 16320258]
7. Lee JH, Lee JE, Kahng JY, Kim SH, Park JS, Yoon SJ, Um J-Y, Kim WK, Lee J-K, Park J, Kim EH, Lee J-H, Lee J-H, Chung W-S, Ju YS, Park S-H, Chang JH, Kang S-G, Lee JH (2018) Human glioblastoma arises from subventricular zone cells with low-level driver mutations. Nature 560: 243–247 doi:10.1038/s41586-018-0389-3 [PubMed: 30069053]
8. Ellingson BM, Lai A, Harris RJ, Selfridge JM, Yong WH, Das K, Pope WB, Nghiemphu PL, Vinters HV, Liau LM, Mischel PS, Cloughesy TF (2013) Probabilistic Radiographic Atlas of Glioblastoma Phenotypes. American Journal of Neuroradiology 34: 533 doi:10.3174/ajnr.A3253 [PubMed: 22997168]
9. Kroonen J, Nassen J, Boulanger Y-G, Provenzano F, Capraro V, Bours V, Martin D, Deprez M, Robe P, Rogister B (2011) Human glioblastoma-initiating cells invade specifically the subventricular zones and olfactory bulbs of mice after striatal injection. International Journal of Cancer 129: 574–585 doi:10.1002/ijc.25709 [PubMed: 20886597]
10. Chen L, Guerrero-Cazares H, Ye X, Ford E, McNutt T, Kleinberg L, Lim M, Chaichana K, Quinones-Hinojosa A, Redmond K (2013) Increased Subventricular Zone Radiation Dose Correlates With Survival in Glioblastoma Patients After Gross Total Resection. International Journal of Radiation Oncology*Biology*Physics 86: 616–622 doi:10.1016/j.ijrobp.2013.02.014
11. Weinberg BD, Boreta L, Braunstein S, Cha S (2018) Location of subventricular zone recurrence and its radiation dose predicts survival in patients with glioblastoma. J Neurooncol 138: 549–556 doi:10.1007/s11060-018-2822-8 [PubMed: 29546530]
12. Maier SE, Sun Y, Mulkern RV (2010) Diffusion imaging of brain tumors. NMR Biomed 23: 849–864 doi:10.1002/nbm.1544 [PubMed: 20886568]
13. Ellingson BM, Malkin MG, Rand SD, Connelly JM, Quinsey C, LaViolette PS, Bedekar DP, Schmainda KM (2010) Validation of functional diffusion maps (fDMs) as a biomarker for human glioma cellularity. J Magn Reson Imaging 31: 538–548 doi:10.1002/jmri.22068 [PubMed: 20187195]
14. Chenevert TL, Stegman LD, Taylor JM, Robertson PL, Greenberg HS, Rehemtulla A, Ross BD (2000) Diffusion magnetic resonance imaging: an early surrogate marker of therapeutic efficacy in brain tumors. J Natl Cancer Inst 92: 2029–2036 doi:10.1093/jnci/92.24.2029 [PubMed: 11121466]
15. Karavaeva E, Harris RJ, Leu K, Shabihkhani M, Yong WH, Pope WB, Lai A, Nghiemphu PL, Liau LM, Chen W, Czernin J, Cloughesy TF, Ellingson BM (2015) Relationship Between [18F]FDOPA PET Uptake, Apparent Diffusion Coefficient (ADC), and Proliferation Rate in Recurrent Malignant Gliomas. Mol Imaging Biol 17: 434–442 doi:10.1007/s11307-014-0807-3 [PubMed: 25465392]
16. Chang W, Pope WB, Harris RJ, Hardy AJ, Leu K, Mody RR, Nghiemphu PL, Lai A, Cloughesy TF, Ellingson BM (2015) Diffusion MR Characteristics Following Concurrent Radiochemotherapy Predicts Progression-Free and Overall Survival in Newly Diagnosed Glioblastoma. Tomography 1: 37–43 doi:10.18383/j.tom.2015.00115 [PubMed: 26740971]
17. Durand-Muñoz C, Flores-Alvarez E, Moreno-Jimenez S, Roldan-Valadez E (2019) Pre-operative apparent diffusion coefficient values and tumour region volumes as prognostic biomarkers in glioblastoma: correlation and progression-free survival analyses. Insights Imaging 10: 36–36 doi:10.1186/s13244-019-0724-8 [PubMed: 30887267]
18. Elson A, Bovi J, Siker M, Schultz C, Paulson E (2015) Evaluation of absolute and normalized apparent diffusion coefficient (ADC) values within the post-operative T2/FLAIR volume as

adverse prognostic indicators in glioblastoma. J Neurooncol 122: 549–558 doi:10.1007/s11060-015-1743-z [PubMed: 25700835]

19. Asao C, Korogi Y, Kitajima M, Hirai T, Baba Y, Makino K, Kochi M, Morishita S, Yamashita Y (2005) Diffusion-Weighted Imaging of Radiation-Induced Brain Injury for Differentiation from Tumor Recurrence. American Journal of Neuroradiology 26: 1455 [PubMed: 15956515]
20. Chatterjee AR, Cachia D, Frankel BM, Giglio P, Das A, Patel SJ (2016) NIMG-19. DIFFUSION KURTOSIS IMAGING OF THE SUBVENTRICULAR ZONE IN GLIOBLASTOMA. Neuro Oncol 18: vi128–vi128 doi:10.1093/neuonc/now212.531
21. Prust MJ, Jafari-Khouzani K, Kalpathy-Cramer J, Polaskova P, Batchelor TT, Gerstner ER, Dietrich J (2015) Standard chemoradiation for glioblastoma results in progressive brain volume loss. Neurology 85: 683 doi:10.1212/WNL.0000000000001861 [PubMed: 26208964]
22. Ellingson BM, Bendszus M, Boxerman J, Barboriak D, Erickson BJ, Smits M, Nelson SJ, Gerstner E, Alexander B, Goldmacher G, Wick W, Vogelbaum M, Weller M, Galanis E, Kalpathy-Cramer J, Shankar L, Jacobs P, Pope WB, Yang D, Chung C, Knopp MV, Cha S, van den Bent MJ, Chang S, Yung WK, Cloughesy TF, Wen PY, Gilbert MR, Jumpstarting Brain Tumor Drug Development Coalition Imaging Standardization Steering C (2015) Consensus recommendations for a standardized Brain Tumor Imaging Protocol in clinical trials. Neuro Oncol 17: 1188–1198 doi:10.1093/neuonc/nov095 [PubMed: 26250565]
23. Cox RW (1996) AFNI: software for analysis and visualization of functional magnetic resonance neuroimages. Comput Biomed Res 29: 162–173 [PubMed: 8812068]
24. van Dijken BRJ, Yan J-L, Boonzaier NR, Li C, van Laar PJ, van der Hoorn A, Price SJ (2017) Subventricular Zone Involvement Characterized by Diffusion Tensor Imaging in Glioblastoma. World Neurosurgery 105: 697–701 doi:10.1016/j.wneu.2017.06.075 [PubMed: 28642175]
25. Ellingson BM, Sahebjam S, Kim HJ, Pope WB, Harris RJ, Woodworth DC, Lai A, Nghiemphu PL, Mason WP, Cloughesy TF (2014) Pretreatment ADC histogram analysis is a predictive imaging biomarker for bevacizumab treatment but not chemotherapy in recurrent glioblastoma. AJNR Am J Neuroradiol 35: 673–679 doi:10.3174/ajnr.A3748 [PubMed: 24136647]
26. Pope WB, Qiao XJ, Kim HJ, Lai A, Nghiemphu P, Xue X, Ellingson BM, Schiff D, Aregawi D, Cha S, Puduvalli VK, Wu J, Yung WK, Young GS, Vredenburgh J, Barboriak D, Abrey LE, Mikkelsen T, Jain R, Paleologos NA, Lada P, Prados M, Goldin J, Wen PY, Cloughesy T (2012) Apparent diffusion coefficient histogram analysis stratifies progression-free and overall survival in patients with recurrent GBM treated with bevacizumab: a multi-center study. J Neurooncol 108: 491–498 doi:10.1007/s11060-012-0847-y [PubMed: 22426926]
27. Ellingson BM, Cloughesy TF, Zaw T, Lai A, Nghiemphu PL, Harris R, Lalezari S, Wagle N, Naeini KM, Carrillo J, Liau LM, Pope WB (2012) Functional diffusion maps (fDMs) evaluated before and after radiochemotherapy predict progression-free and overall survival in newly diagnosed glioblastoma. Neuro Oncol 14: 333–343 doi:10.1093/neuonc/nor220 [PubMed: 22270220]
28. Liu K, Ma Z, Feng L (2018) Apparent diffusion coefficient as an effective index for the therapeutic efficiency of brain chemoradiotherapy for brain metastases from lung cancer. BMC Med Imaging 18: 30–30 doi:10.1186/s12880-018-0275-3 [PubMed: 30223786]
29. Cherubini A, Spoletini I, Péran P, Luccichenti G, Di Paola M, Sancesario G, Gianni W, Giubilei F, Bossù P, Sabatini U, Caltagirone C, Spalletta G (2010) A multimodal MRI investigation of the subventricular zone in mild cognitive impairment and Alzheimer's disease patients. Neuroscience Letters 469: 214–218 doi:10.1016/j.neulet.2009.11.077 [PubMed: 19962428]
30. Achanta P, Capilla-Gonzalez V, Purger D, Reyes J, Sailor K, Song H, Garcia-Verdugo JM, Gonzalez-Perez O, Ford E, Quinones-Hinojosa A (2012) Subventricular Zone Localized Irradiation Affects the Generation of Proliferating Neural Precursor Cells and the Migration of Neuroblasts. STEM CELLS 30: 2548–2560 doi:10.1002/stem.1214 [PubMed: 22948813]
31. Mineyeva OA, Bezriadnov DV, Kedrov AV, Lazutkin AA, Anokhin KV, Enikolopov GN (2019) Radiation Induces Distinct Changes in Defined Subpopulations of Neural Stem and Progenitor Cells in the Adult Hippocampus. Front Neurosci 12: 1013–1013 doi:10.3389/fnins.2018.01013 [PubMed: 30686979]
32. Vlashi E, McBride WH, Pajonk F (2009) Radiation responses of cancer stem cells. J Cell Biochem 108: 339–342 doi:10.1002/jcb.22275 [PubMed: 19623582]

33. Szerlip N, Rutter C, Ram N, Yovino S, Kwok Y, Maggio W, Regine WF (2011) Factors impacting volumetric white matter changes following whole brain radiation therapy. J Neurooncol 103: 111–119 doi:10.1007/s11060-010-0358-7 [PubMed: 20725847]

34. Apple DM, Solano-Fonseca R, Kokovay E (2017) Neurogenesis in the aging brain. Biochemical Pharmacology 141: 77–85 doi:10.1016/j.bcp.2017.06.116 [PubMed: 28625813]

35. Falconer JC, Narayana PA (1997) Cerebrospinal fluid-suppressed high-resolution diffusion imaging of human brain. Magn Reson Med 37: 119–123 doi:10.1002/mrm.1910370117 [PubMed: 8978640]

36. Cloughesy T, Finocchiaro G, Belda-Iniesta C, Recht L, Brandes AA, Pineda E, Mikkelsen T, Chinot OL, Balana C, Macdonald DR, Westphal M, Hopkins K, Weller M, Bais C, Sandmann T, Bruey JM, Koeppen H, Liu B, Verret W, Phan SC, Shames DS (2017) Randomized, Double-Blind, Placebo-Controlled, Multicenter Phase II Study of Onartuzumab Plus Bevacizumab Versus Placebo Plus Bevacizumab in Patients With Recurrent Glioblastoma: Efficacy, Safety, and Hepatocyte Growth Factor and O(6)-Methylguanine-DNA Methyltransferase Biomarker Analyses. J Clin Oncol 35: 343–351 doi:10.1200/jco.2015.64.7685 [PubMed: 27918718]

37. Hartmann C, Hentschel B, Simon M, Westphal M, Schackert G, Tonn JC, Loeffler M, Reifenberger G, Pietsch T, von Deimling A, Weller M (2013) Long-Term Survival in Primary Glioblastoma With Versus Without Isocitrate Dehydrogenase Mutations. Clinical Cancer Research 19: 5146 doi:10.1158/1078-0432.CCR-13-0017 [PubMed: 23918605]

38. Malyarenko DI, Newitt D, J Wilmes L, Tudorica A, Helmer KG, Arlinghaus LR, Jacobs MA, Jajamovich G, Taouli B, Yankeelov TE, Huang W, Chenevert TL (2016) Demonstration of nonlinearity bias in the measurement of the apparent diffusion coefficient in multicenter trials. Magnetic resonance in medicine 75: 1312–1323 doi:10.1002/mrm.25754 [PubMed: 25940607]

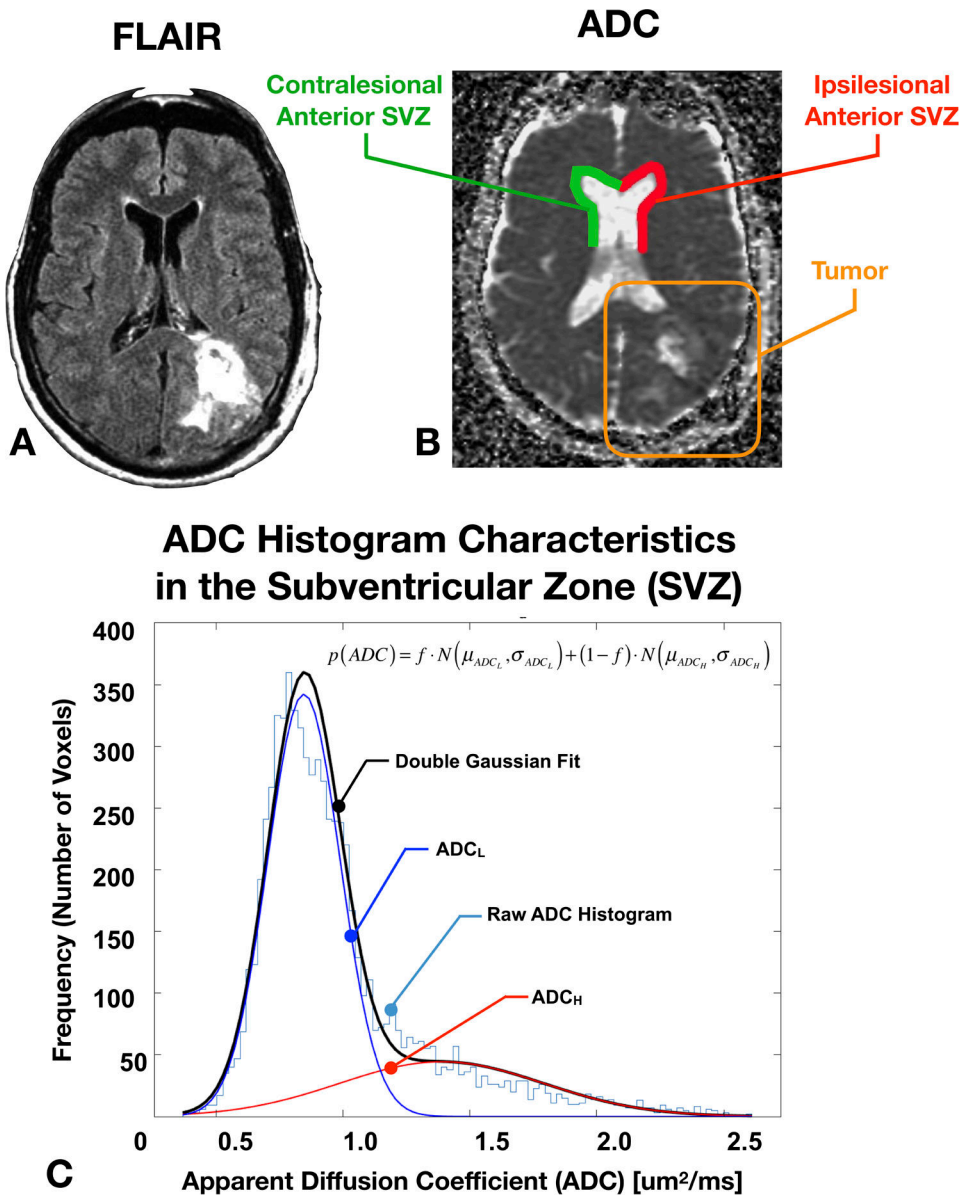

Fig. 1: Subventricular zone (SVZ) region of interest (ROI) selection and ADC histogram analysis methodology.

A) FLAIR image from a representative glioblastoma patient showing a lesion in the left occipital lobe. B) Diagram illustrating the ipsilesional (red) and contralesional (green) ROIs relative to the location of the primary lesion (orange). C) ADC histogram analysis using a double Gaussian mixed model. ADC_L and ADC_H are defined as the lower and higher mean value of this bimodal distribution.

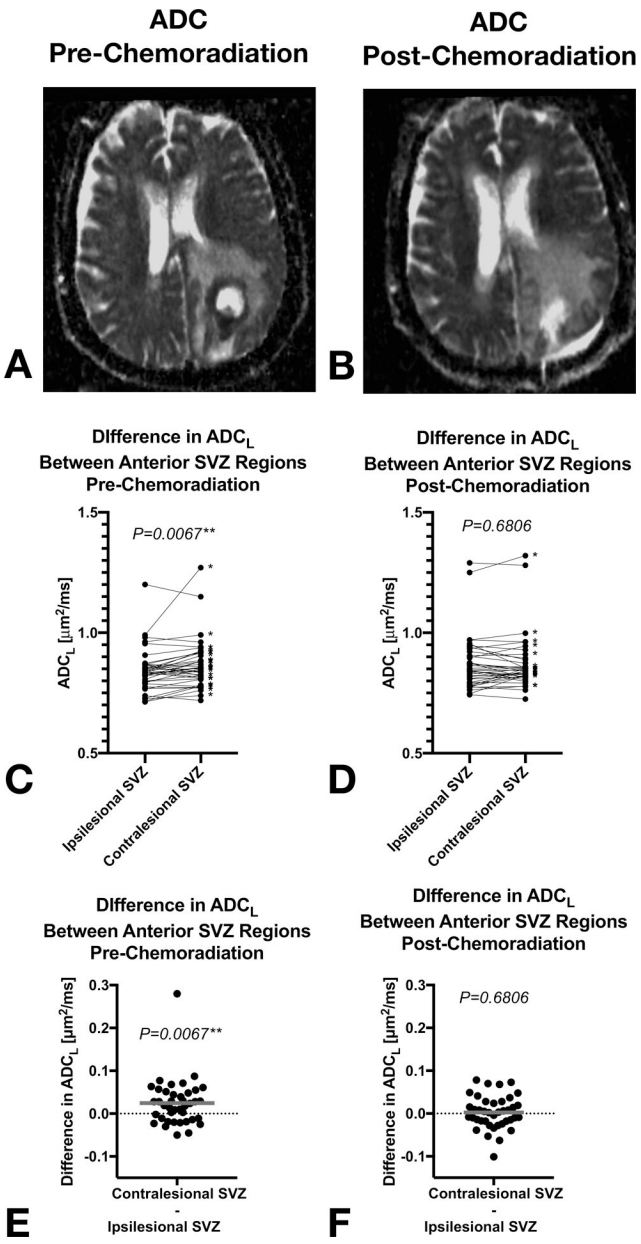

Fig. 2: Comparison between ADC_L in the ipsilesional and contralesional SVZ pre- and post-chemoradiation in newly diagnosed glioblastoma.

A) Pre- and B) post-chemoradiation ADC map in a patient with a left occipital glioblastoma. C) Comparison of ADC_L between anterior ipsilesional and contralesional SVZ regions prior to chemoradiation. D) Comparison of ADC_L between anterior ipsilesional and contralesional SVZ regions after to chemoradiation. E) Difference in ADC_L between anterior ipsilesional and contralesional SVZ regions prior to chemoradiation. F) Difference in ADC_L between anterior ipsilesional and contralesional SVZ regions after to chemoradiation.

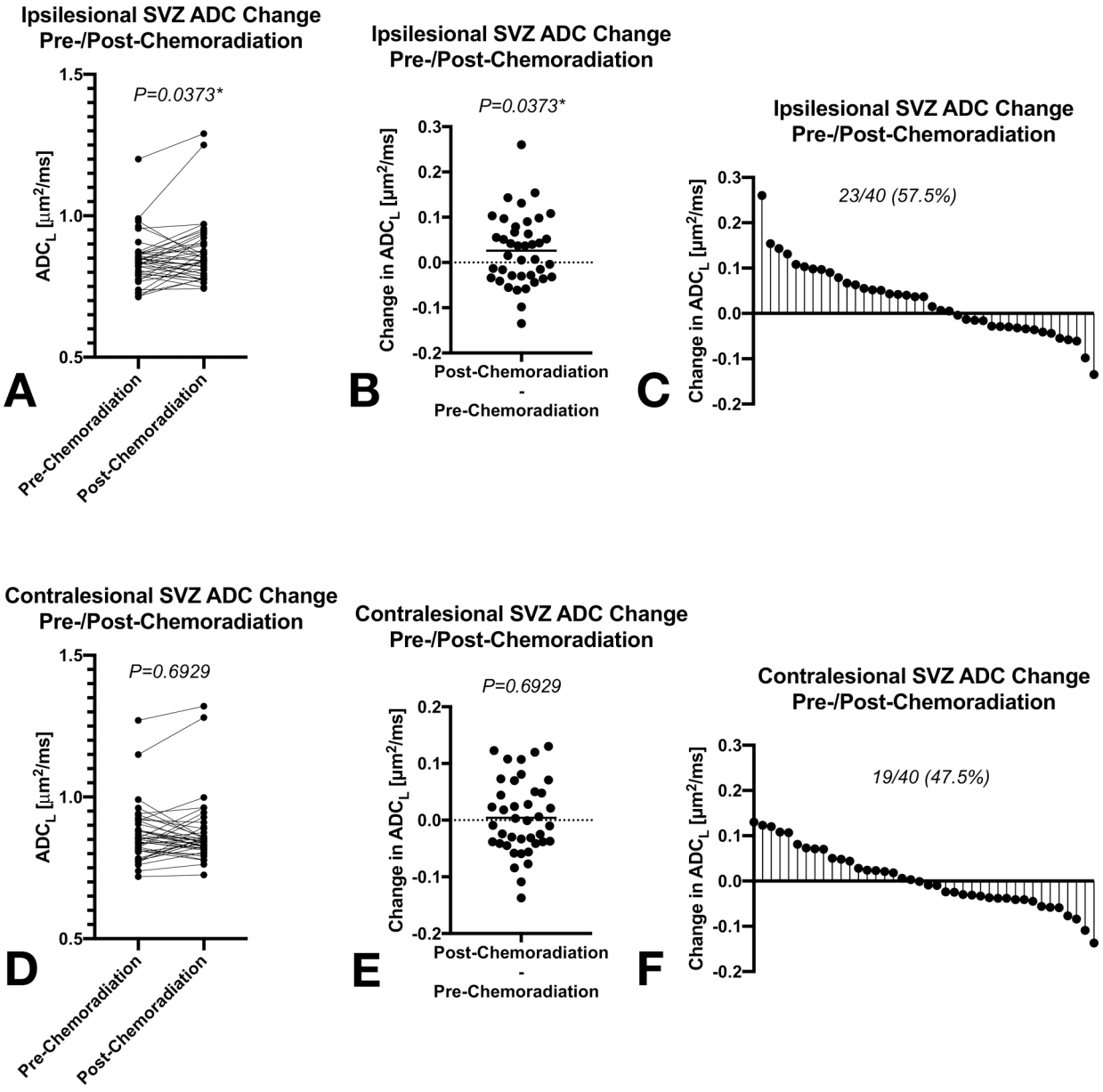

Fig. 3: Changes in ADC_L within the ipsilesional and contralesional SVZ after chemoradiation.

A) Ipsilesional ADC_L measurements pre- and post-chemoradiation. B) Change in ADC_L within the ipsilesional SVZ after chemoradiation. C) Waterfall plot showing distribution of change in ADC_L within the ipsilesional SVZ for the study population. D) Contralesional ADC_L measurements pre- and post-chemoradiation. E) Change in ADC_L within the contralesional SVZ after chemoradiation. F) Waterfall plot showing distribution of change in ADC_L within the contralesional SVZ for the study population.

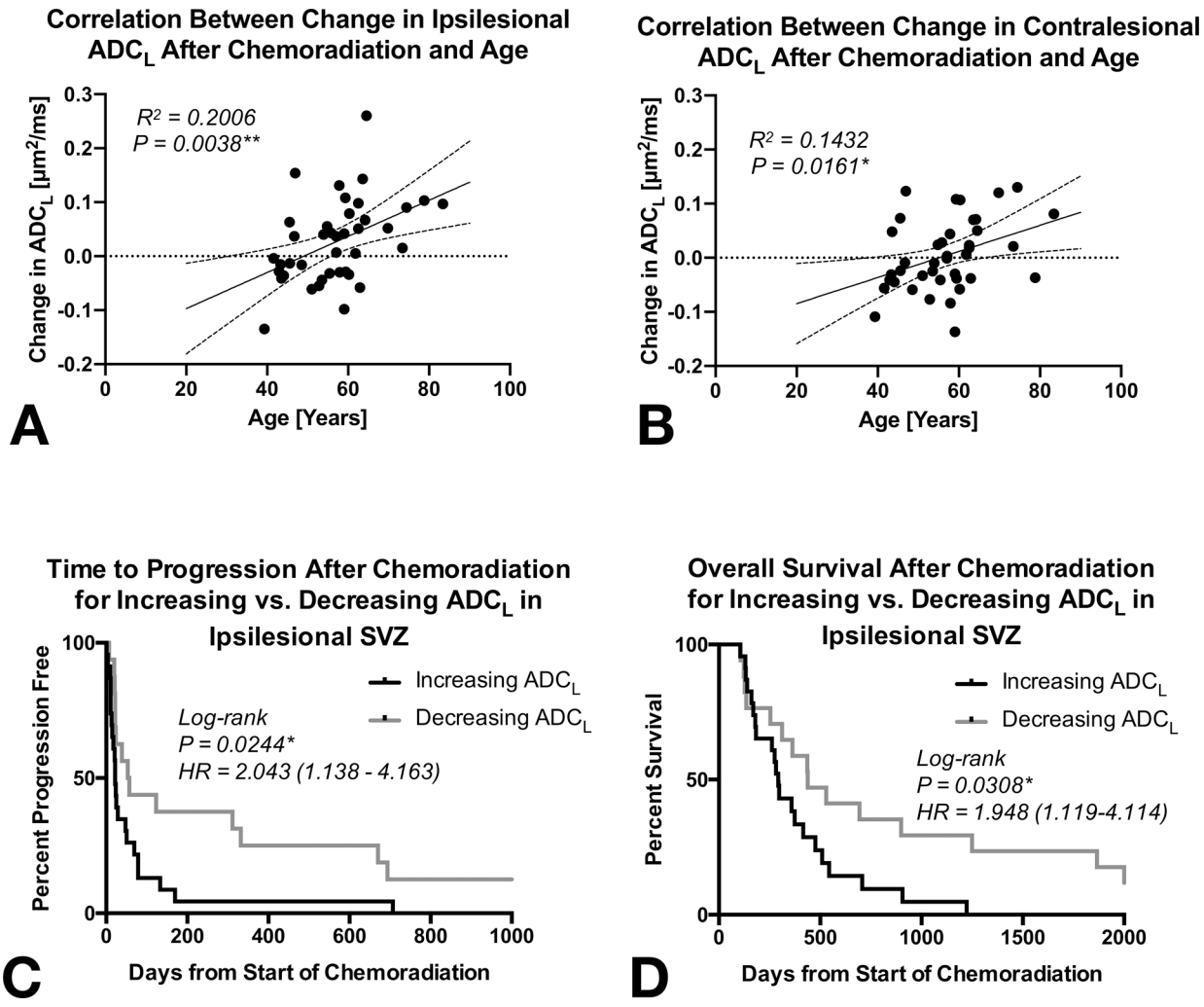

Fig 4: Relationship between change in ADC$_L$ after chemoradiation, patient age, and outcome.

A) Correlation between change in ADC$_L$ in the ipsilesional SVZ and patient age. B) Correlation between change in ADC$_L$ in the contralesional SVZ and patient age. C) Comparison of time to progression after chemoradiation between patients with increasing versus decreasing ADC$_L$ within the ipsilesional SVZ. D) Comparison of overall survival after chemoradiation between patients with increasing versus decreasing ADC$_L$ within the ipsilesional SVZ.

Table 1.

Patient Demographics

Characteristics	All Patients (n=40)	Left-Hemispheric Tumor Patients (n=25)	Right-Hemispheric Tumor Patients (n=15)
Sex (Male/Female)	26/14	17/8	9/6
Average Age (Years) ± SD	57 ± 10	59 ± 11	53 ± 8
Overall Survival (Days) ± SD	622 ± 805	386 ± 342	1016 ± 1158
Progression-Free Survival (Days) ± SD	265 ± 757	92 ± 156	554 ± 1189
Average Days Between Pre-/Post-RT Scans ± SD	80 ± 22	77 ± 20	90 ± 23

Table 2.

Multivariable Cox Regression Results for Progression-Free Survival (PFS) Using Patient Age, Hemisphere of Tumor Involvement, Change in ADC_L, and the Interaction Between Hemisphere and Change in ADC_L within the Ipsilesional SVZ.

Variable	Coefficient	Hazard Ratio (HR)	P-Value
Age	−0.0075	0.9922 (0.9507–1.0355)	0.7195
Hemispheric Involvement (Left/Right)	0.1443	1.1553 (0.5701 – 2.3411)	0.6888
Increase vs. Decrease in ADC_L in the Ipsilesional SVZ	1.4618	4.3138 (1.2160 – 15.3035)	0.0237*
Interaction Between Hemisphere and Increase/Decrease in ADC_L	−0.6628	0.5154 (0.2485 – 1.0691)	0.0750

Table 3.

Multivariable Cox Regression Results for Overall Survival (OS) Using Patient Age, Hemisphere of Tumor Involvement, and Change in ADC_L within the Ipsilesional SVZ.

Variable	Coefficient	Hazard Ratio (HR)	P-Value
Age	−0.0087	0.9913 (0.9559–1.0280)	0.6388
Hemispheric Involvement (Left/Right)	0.8744	2.3974 (1.0985 – 5.2325)	0.0281*
Increase vs. Decrease in ADC_L in the Ipsilesional SVZ	0.9515	2.5895 (0.6677–10.0434)	0.1689
Interaction Between Hemisphere and Increase/Decrease in ADC_L	−0.3818	0.6826 (0.3181–1.4647)	0.3270